Study of $\mathcal{PT}$-symmetric Lattice Hamiltonians

Kokkimidis Patatoukos

University of Crete,

Physics Department

Supervisor: Theodore Tomaras

Master Thesis

Heraklion 2017

Acknowledgements

For the completion of the present thesis I would like to thank Professor Konstantinos Makris for his continuous guidance and immense amount of help. Not only for the present work but also for helping me sort out things regarding my future in Physics. I would also like to thank Professor Theodore Tomaras for fruitful conversations on the topic of the present thesis and his patience in teaching me Physics during the course of my graduate and undergraduate studies. Finally, I would like to thank my parents for their continuous support, because without them I wouldn't be able to finish the present thesis.

Abstract

In the following thesis a study of non-Hermitian $\mathcal{PT}$-symmetric lattice Hamiltonians is presented. In 1998, it has been discovered by Bender et.al [1][2][3], that $\mathcal{PT}$-symmetric operators however non-Hermitian, have completely or partially real eigenvalue spectrum. We focus our attention to the study of Hamiltonian operators that are $\mathcal{PT}$-symmetric and show how one can predict the reality or complexity of the spectrum and the point of transition to the so-called *broken* $\mathcal{PT}$ *phase*, where the eigenvalues become complex. After that there is also a numerical study of various $\mathcal{PT}$-symmetric Hamiltonians in which their eigenvalue spectrum and band structure is investigated as the spatial frequency of the imaginary potential increases. Moreover,wavepacket diffraction has been studied in these lattices. One can discern the interesting and counter intuitive ideas of the $\mathcal{PT}$ symmetry in wave propagation dynamics. It is quite interesting the fact that however non-Hermitian some Hamiltonians have a completely real eigenvalue spectrum, which is considered to be a trait of the $\mathcal{PT}$-symmetry. This fact helps us bypass one of the axioms of Quantum Mechanics which is that the operators that represent physical quantities must be hermitian.

Contents

Chapter 1

Introduction

One of the axioms of Quantum Mechanics is that physical quantities are represented by linear hermitian operators which act on a Hilbert space. And what is physically measurable is the expectation values of these operators in the state that describes our system. Because what we measure is real we want those expectation values to be real. The problem is that the states that describe the systems in Quantum Mechanics are pure phases, which means they are complex, in general. Since the expectation values are connected with the eigenvalues of the operators, physicists had to find operators that have real eigenvalues. Such operators exist and are called Hermitian operators which by definition obey the condition $\hat{O}^\dagger = (\hat{O}^*)^T = \hat{O}$ *i.e.* the complex conjugate and transpose operator is the same as the operator. This condition ensures the reality of the eigenvalues of the operator. However, in 1998, Bender *et al.*[1] have shown that it is in fact possible for operators that are non-Hermitian to have a completely real eigenvalue spectrum as long as they are $\mathcal{P}$-parity and $\mathcal{T}-time$-symmetric. This result appears to be fascinatingly counter-intuitive since conventional Quantum Mechanics do not work. Another fascinating characteristic of a system with such symmetry, is the spontaneous $\mathcal{PT}$ symmetry breaking beyond which this class of systems undergo a phase transition where the system loses its $\mathcal{PT}$ property and some of the eigenvalues become complex. The notion of $\mathcal{PT}$ symmetry is considered in many diverse areas of physics today, such as lattice QCD, optics and other active research areas.

When we say that an operator is $\mathcal{PT}$-symmetric we only mean that, that operator commutes with the $\mathcal{PT}$-operator. This does not mean that the eigenfunctions of such operator are also eigenfunctions of the $\mathcal{PT}$ operator. This is because time inversion operator is not linear as is required by the QM axiom. The action of the $\mathcal{PT}$ operator is defined as the combined action of the parity operator $\mathcal{P}$ and the time inversion operator $\mathcal{T}$. Specifically, the action of the parity operator takes $\hat{p} \to -\hat{p}$ and $\hat{x} \to -\hat{x}$ while the time inversion operator takes $\hat{p} \to -\hat{p}$, $\hat{x} \to \hat{x}$ and $i \to -i$ where $\hat{x}$ and $\hat{p}$

are the position and the momentum operators respectively. It is now obvious that a Hamiltonian, which consists of a conventional kinetic term and a potential V, is $\mathcal{PT}$ symmetric if and only if:

$$V(x) = V^*(-x) \tag{1.1}$$

For Eq.(1.1) to hold true we want the real part of the potential to be an even function while the imaginary part to be an odd function of x.

As these counter intuitive ideas were beginning to take shape and were explored in the aforementioned fields, it was shown in [5] that the basic ideas of $\mathcal{PT}$ symmetry can be realized experimentally in the context of photonics. In this framework of PT-optics, the authors of [5] studied the band structure that corresponds to the potential:

$$V(x) = 4cos^2(x) + i4V_0 sin(2x) \tag{1.2}$$

They found, numerically, that there is a critical point V_0 beyond which we have a phase transition and the eigenvalues of the Hamiltonian form complex conjugate pairs. They found that above the critical point, bands merge forming loops within the Brillouin zone while the in the regions where the bands overlap the eigenvalues become complex conjugate pairs and the modes are substantially altered. They also studied the dynamics of wave propagation which lead to power oscillations and double refraction.

It was shown, later, in [6] that the potential in Eq.(1.2) can be transformed and be written in a pseudo-Hermitian form by a similarity transformation. With this method and the notion of the pseudo hermiticity, that was introduced in [7], they showed analytically that there is indeed a critical point V_0 beyond which the symmetry is broken and the eigenvalues become complex as expected.

In this work we are going to study some Lattice Hamiltonians by applying both analytical and computational techniques.

In the second chapter, we will introduce the notion of pseudo hermiticity which was first introduced in[7].

In the third chapter after a short introduction to antiunitary operators and their corepresentations we will be able to better understand the ideas of the following chapter.

In the fourth chapter we analyze the work done by Mock[8] on $\mathcal{PT}$ Lattices group theory.

In the fifth chapter there is an introduction to the ideas behind the numerical methods that were used to obtain the results of the present work.

After all those introductory chapters we will present the main results regarding novel optical non-Hermitian lattices. We will study potentials of the form:

$$V(x) = cos^{2n}(x) + i \sum_{m=1}^{m=2n} V_{2m} sin(2mx) \tag{1.3}$$

and see that there is a line in the parameter space where the potential has completely real eigenvalue spectrum. In the same chapter we will use an example to showcase the transformation and also study optical wave dynamics in the interesting regime which obviously is the unbroken $\mathcal{PT}$ phase.

In the seventh chapter we study potentials with just varying spatial frequency of the imaginary part. We prove in two ways that the higher the frequency of the imaginary part the higher is the order of the band that has complex eigenvalues. Which means that the more physically irrelevant become the complex eigenvalues and thus we can treat them as Hamiltonians with unbroken symmetry.

In the final eighth chapter we summarize our work and discuss how they are related to realistic $\mathcal{PT}$-symmetric photonic systems.

Chapter 2

Pseudo-Hermitian Operators

In 2002, Mostafazadeh[7] introduced the notion of Pseudo-Hermiticity and showed that every non-Hermitian Hamiltonian with a real spectrum is Pseudo-Hermitian. This statement implies that it is not the $\mathcal{PT}$-symmetry that gives the Hamiltonian the property of the real spectrum, but its Pseudo-Hermiticity. However, we know that $\mathcal{PT}$-Hamiltonians are of two kinds. Those which have an exact $\mathcal{PT}$-symmetry which from now on we will call $\mathcal{PT}$-exact Hamiltonians and those who have a phase of broken $\mathcal{PT}$-symmetry which we will call $\mathcal{PT}$-broken from here on. It is one of the properties of the $\mathcal{PT}$ symmetric Hamiltonians that if they are $\mathcal{PT}$-exact then the spectrum is completely real while the $\mathcal{PT}$-broken ones have complex conjugate pairs of eigenvalues. Another property is that the inner product:

$$\langle\langle\psi_2|\psi_1\rangle\rangle_P = \langle\psi_2|P|\psi_1\rangle \tag{2.1}$$

is invariant under time inversion. Note, that the states are eigenstates of the Hamiltonian.

Since we cannot be sure that $\mathcal{PT}$ symmetry is in principle the reason responsible for the reality of the eigenvalue spectrum, we introduce the concept of pseudohermiticity defined as:

- A linear operator O is η-*pseudohermitian* if:

$$O^{\#} := \eta^{-1}O^{\dagger}\eta = O \tag{2.2}$$

  where η is linear positive definite operator.

What the previous definition says is that if the hermitian conjugate of an operator is equal to the original operator up to a similarly transformation then we call it Pseudo-Hermitian. Now using Schroedinger's equation and its Hermitian conjugate along with Eq.(2.2) for the Hamiltonian we see that:

$$\begin{aligned} \left\langle \psi|\eta H - H^\dagger \eta|\psi \right\rangle &= i\partial_t \left\langle \langle \psi|\psi \rangle \right\rangle_\eta \\ H^\dagger \eta &= \eta H \end{aligned} \tag{2.3}$$

So the indefinite inner product is time invariant if the Hamiltonian H is pseudo-hermitian. It should be obvious that in the limit where $\eta = 1$ we have the regular hermiticity condition for an operator. Moreover, a $\mathcal{PT}$ symmetric Hamiltonian:

$$H = \frac{p^2}{2m} + V(x) \tag{2.4}$$

where V(x) obeys Eq.(1.1) is also P pseudohermitian since

$$H^\dagger = pHp^{-1} = pHp \tag{2.5}$$

Now using the second relation of the Eq.(2.3) one can easily show that energy eigenstates are η orthogonal to themselves if their eigenvalues are not real or complex conjugate. This can be seen from

$$\left\langle \psi_i|-\eta H + H^\dagger \eta|\psi_j \right\rangle = (E_i^* - E_j) \left\langle \psi_i|\eta|\psi_j \right\rangle \tag{2.6}$$

There are a lot more properties of the pseudohermitian operators. However, their proof is a simple application of the previous ones and of the definition, and they will not be shown here.

To close this section we will show that pseudohermitian Hamiltonians with discrete spectrum and a complete biorthonormal basis have either real spectrum or complex conjugate pairs of eigenvalues. The previous statements can be formulated like this:

$$\begin{aligned} H\left|n,a\right\rangle = E_n \left|n,a\right\rangle, \quad H^\dagger \left|m,a\right\rangle &= E_m^* \left|m,a\right\rangle \\ \left\langle m,a|n,b\right\rangle &= \delta_{mn}\delta_{ab} \\ \sum_{n,a} \left|n,a\right\rangle \left\langle n,a\right| &= 1 \end{aligned} \tag{2.7}$$

where a and b are degeneracy indices From these relations and the second part of Eq.(2.3) it's now straight forward exercise to show that

$$H(\eta^{-1}\left|n,a\right\rangle) = \eta^{-1} H^\dagger \left|n,a\right\rangle = E_n^*(\eta^{-1}\left|n,a\right\rangle) \tag{2.8}$$

To prove the proposition the other way around we just deconstruct our Hamiltonian in real energy states and states with positive and negative imaginary part. Using Eq.(2.7) one can construct the η in terms of the basis states. Then one can show that the formulae we get for the Hamiltonian and the η satisfy the second relation of Eq.(2.3). We will, later on, use this notion on a simple potential to find out where in the parameter space the eigenvalues of the Hamiltonian are real.

Chapter 3

Antiunitary Operators

Within the framework of quantum mechanics we are mostly interested in unitary operators. And that is completely comprehensible since we want the operators to preserve the norm. That is to say we want our operators to preserve the probability. Conservation of probability is one of the most basic ideas of Quantum Mechanics. However, the $\mathcal{PT}$ operator is not unitary. Although, parity operator may be unitary since $\mathcal{P}^2 = 1$ the time reversal operator is not. The $\mathcal{T}$ operator is antiunitary. To better understand antiunitarity consider two operators that act as below:

$$\mathcal{L} := t \to t + \tau \tag{3.1}$$

$$\mathcal{T} := t \to -t \tag{3.2}$$

Now if we first perform a time reversal and then a time translation by τ we will be at time $-t + \tau$. However if we do the same thing but reverse the order of the operators we will be at time $-t - \tau$. This means that:

$$(\mathcal{L}) \times (\mathcal{T}) = (\mathcal{T}) \times (-\mathcal{L}) \tag{3.3}$$

Which is exactly the antiunitary character of the time reversal operator in action.

Now assume that the $\mathcal{T}$ operator is linear and a symmetry operator of a given system. Then if we have a state in the form: $\Phi_0 = \sum_k a_k \psi_k$, where ψ_k are the eigenvectors f the Hamiltonian of the system, the linearity of $\mathcal{T}$ would suggest $\mathcal{T}\Phi_0 = \sum_k a_k \mathcal{T}\psi_k$ and since it is a stationary state with the same energy as the one written before, then the time evolved state will be:

$$\mathcal{T}\Phi_0 = \sum_k a_k e^{-iE_k t/\bar{h}} \mathcal{T}\psi_k \tag{3.4}$$

However this should be the same state as obtained from acting with the time reversal operator on the state: Φ_{-t}:

$$\mathcal{T}\Phi_{-t} = \sum_k a_k e^{iE_k t/\bar{h}} \mathcal{T}\psi_k \tag{3.5}$$

As you can see the Eqs.(3.4) and (3.5) are not consistent with each other.

To fix the problem we would very much like to have:

$$\mathcal{T}\Phi_0 = \sum_k a_k^* \mathcal{T}\psi_k \tag{3.6}$$

Operators that obey the Eq.(3.6) we call them *antilinear*. However, time reversal is still a symmetry operator, which means it should leave the transition probability between two states invariant, which means:

$$|(\Phi, \Psi)| = |(\mathcal{T}\Phi, \mathcal{T}\Psi)| \tag{3.7}$$

If an operator obeys simultaneously the Eqs(3.6) and (3.7) we call it antiunitary. There are many properties of these kind of operators that we could write down. For example, every antiunitary operator can be written in a product form between a unitary operator and the anti unitary operator of the complex conjugation.

$$\mathcal{T} = UC \tag{3.8}$$

The time inversion operator has the additional property that if we act 2 times on a state we will get the same state. Hence, the new state can differ from the first only by a constant factor. This factor can be ± 1. This can be seen if one writes $\mathcal{T} = UC$ then we have $\mathcal{T}^2 = UCUC = UCCU^* = UU^* = \pm 1$ since U is unitary.

When a group contains both unitary and antiunitary operators we would have a problem in finding the groups representations. If a group contains both kinds of operators, the set of the unitary operators form a subgroup of that group while the antiunitary operators will form a coset of the subgroup (Eq.(3.8)).

The problem that we mentioned before is that since we have antilinear operator its matrix representation must obey antilinear relations which means that the usual relations for the representations: $D(\mathcal{T}O_U O_V) = D(\mathcal{T}O_{UV})$ do not hold. Instead, we should have:

$$D(\mathcal{T}O_U)D(O_V)^* = D(\mathcal{T}O_U O_V) \tag{3.9}$$

We call matrices that obey Eq.(3.9) corepresentations. Obviously the notion of corepresentations applies only to a group which contains both kinds of operators mentioned before.

Now we have to somehow find the irreducible corepresentations of the group. Which is translated to finding the solutions of equations like the one in (3.9). Equivalent solutions are called the solutions that are related to each other with the following transformation:

$$\begin{aligned} \bar{D}(U) &= A_0^{-1} D(U) A_0 \\ \bar{D}(A) &= A_0^{-1} D(A) A_0^* \end{aligned} \tag{3.10}$$

where A_0 is a unitary matrix while A is antiunitary. If they are a multiple of the identity then the transformation of the matrices of the unitary operators remain the same while the matrices of the antiunitary matrices differ by a numerical factor. Suppose we know the representation of the unitary subgroup and we denote them as: $\Delta(u)$. Note that $\Delta(a)$ is meaningless to write down since a is an antiunitary operator. However $\Delta(a_1 a_2)$ and $\Delta(a^{-1}ua)$ are well defined since these operators are unitary and we can write them down.

Let us assume that D(u) as a representation of the unitary subgroup has been completely reduced and that the dimension is l:

$$u\psi_k = \sum_1^l \Delta(u)_{km}\psi_m \tag{3.11}$$

for k less than l. We now define the primed wavefunctions which are the normal wavefunctions but we act on those l wave functions with an antiunitary operator a

$$\psi'_k = a\psi_k = \sum_1^f D(a)\psi \tag{3.12}$$

We shall show that the primed wavefunctions belong to an irreducible representation of the unitary subgroup:

$$u\psi'_k = \sum_m \left[D(u)D(a)\right]_{mk}\psi_m = \sum_m D(ua)\psi = \sum_m D(a)D(a^{-1}ua)^*\psi = \sum_m D(a)\Delta(a^{-1}ua)^*\psi \tag{3.13}$$

We can see that these matrices form a different representation of the unitary subgroup:

$$\bar{\Delta}(u) = \Delta(a^{-1}ua)^* \tag{3.14}$$

Note that the similar relations hold true for $\Delta(a_1 a_2)$

It is the relation between the barred and the unbarred representation that will help us in our case.

It can be shown that the primed wavefunctions can all be written as a linear combination of the l linearly independent wavefunctions of the irreducible representations of the unitary subgroup or are all linearly independent.

In the first case: it follows that $u\psi_k$ and $a\psi_k$ are linear combinations of these l functions. In this case the corepresentation is reduced to an l-dimensional and to an $(f-l)$-dimensional part.

In the second case: the corepresentation will have 2 parts with the first if them being of dimension $2l$ and the second one $f-2l$. Where the first $2l$-dimensional irreducible first part will contain both Δ and $\bar{\Delta}$

So we arrive at the conclusion that every reduced part of the corepresentation will contain:

- only one irreducible representation
- or only two, Δ and $\bar{\Delta}$

Finally, let us take a look in the relation between the two irreducible representations that we found.

There are two possibilities, that the corepresentations are inequivalent and equivalent. However, the case when these two are equivalent is more complicated.

- inequivalent

  If $\Delta(u)$ and $\Delta(a^{-1}ua)^*$ are inequivalent then this means that the l wavefunctions are orthogonal to the l primed wavefunctions and thus the matrices can be written in the form:

$$D(u) = \begin{bmatrix} \Delta(u) & 0 \\ 0 & \Delta(a^{-1}ua)^* \end{bmatrix} \tag{3.15}$$

$$D(a) = \begin{bmatrix} 0 & \Delta(aa_0) \\ \Delta(a_0^{-1}a) & 0 \end{bmatrix} \tag{3.16}$$

- equivalent

  In this situation the two are related with (3.10) $\beta^{-1}\Delta(u)\beta = \bar{\Delta}(u)$. There are two cases to be distinguished: the representation D and Δ may have the same dimension or double the dimension of Δ. In both cases it is trivial to write down D(u). However we have to see what happens on the D(a) Using the equivalence transformation (3.10) twice on a unitary matrix we get:

$$\Delta(a^{-2})\Delta(u)\Delta(a^2) = \Delta(a^{-2}ua^2) = \beta^{-1*}\beta\Delta(u)\beta\beta^*$$

It follows that the matrix $\beta\beta^*\Delta(a^{-2})$ commutes with all of the matrices of the representation of the unitary subgroup. And thus its a multiple of a number a. However since all matrices are unitary this number can only be ± 1. Hence we have:

$$\begin{aligned} \beta\beta^* &= \Delta(a^2) \\ \beta\beta^* &= -\Delta(a^2) \end{aligned} \tag{3.17}$$

It is clear that for each case discussed above we have a difference in the corepresentation of the antiunitary operators in the case of plus or minus. For example in the case of plus(minus):

1. $\beta = D(a)$ $(\Delta(aa_0^{-1})\beta = D(a))$

2. $\beta \times E_{2x2} = D(a)$ $(\Delta(aa_0^{-1})\beta \times C_{2x2} = D(a))$ Where E is the 2 by 2 identity matrix and C is the 2 by 2 skew symmetric matrix with elements 1 and -1.

To summarize we have 3 types of irreducible corepresentations. The type (a) where the dimension of D and Δ is the same and Δ is equivalent with $\bar{\Delta}$, the type (b) where the dimension of D is double that of Δ and also Δ is equivalent with $\bar{\Delta}$ and finally the type(c) where the barred and the unbarred representations are not equivalent.

As a final remark we note that the irreducible parts of the corepresentations are determined by the irreducible representations of the unitary subgroup. Which means that the character of the representation of the unitary subgroup is the criterion that determines which one of the three types our problem falls into.

Chapter 4

Group Theory in $\mathcal{PT}$-Lattices

One of the initial motivations of this thesis was to find a group theoretical way to classify the $\mathcal{PT}$ Hamiltonians. That is to say that we wanted to find a general behaviour of the eigenvalue spectrum of a given Hamiltonian purely based on the symmetry operations that leave the system invariant.

In 2016 Mock [8] made some steps forward in this direction, using the formalism we just showcased. In this chapter we will present his work and assumptions. Finally, we will make some comments on the results that come to contradict some of his statements.

Let us consider a $\mathcal{PT}$-symmetric system. It is quite well known ([1], [5]) that the eigenvalues of the Hamiltonian that governs our system has real or pairs of complex conjugate eigenvalues. In general, we have two categories of Hamiltonians depending on the reality of the eigenvalue spectrum. The Hamiltonians whose spectrum remains real as we turn on the non-Hermiticity factor but become complex after a critical point, and the Hamitlonians whose spectrum becomes complex at the moment we turn on the non-Hermiticity. We call the Hamiltonians of the second kind thresholdless, because there is not a threshold up to which our $\mathcal{PT}$-symmetry is not broken. According to Mock's study the precise spatial symmetry of the non Hermitian potential determines the reality or complexity of the eigenvalues in the thresholdless case. In his work he used a one dimensional electromagnetic periodic structure with alternating gain and loss. Since the gain and loss appear in the Maxwell equations as a complex index of refraction $n = n_r \pm in_i$ where the plus is for gain or loss depending on the Fourier convention used. He solved the electromagnetic wave equation in a source-free non-magnetic medium with n_r constant and n_i a constant with alternating sign periodically. Considering that a cell of the lattice is of length Λ and in that cell the gain and loss is equally distributed in the first half($\frac{\Lambda}{2}$) and in the second half of the cell accordingly we can now write down all the symmetry operators- elements

that leave the structure invariant. These are $e = \{E|0\}$, $m = \{\sigma|0\}$, $\xi = \{T|\Lambda/2\}$ and $\mu = \{\mathcal{T}\sigma|\Lambda/2\}$where the first part describes a group operation and the second part describes a translation by the amount in the bracket. Obviously E stands for the identity element, σ is a reflection and $\mathcal{T}$ is an inversion of gain and loss (or time inversion). The first two operators do not include time reversal so they are unitary. However the last two contain $\mathcal{T}$ and thus they are antiunitary. Hence, the unitary subgroup is of index 2.

Before we go on note that since $\xi\xi$ is a pure translation we will have to use the full space group. Thankfully the Bloch theorem constrains the form of the modes of periodic systems and we can use the representation of the space group $exp(ikn\Lambda)$

As we mentioned before as a final remark on the previous chapter the irreducible parts of the corepresentations are determined by the irreducible representations of the unitary subgroup. Which means that the character of the representation of the unitary subgroup is the criterion that determines which one of the three types our problem falls into. To help us determine the category of the corepresentations Frobenius and Shur developed a test (Frobenius-Shur Lemma) which is:

$$\sum_{B\in\mathcal{W}} \chi(B^2) = \begin{cases} n, & Type \ \ (a) \\ -n, & Type \ \ (b) \\ 0, & Type \ \ (c) \end{cases} \tag{4.1}$$

where $\chi(B)$ is the character of the representation of the operator B and n is the index of the unitary subgroup while $\mathcal{W}$ is the set of the antiunitary operators. Type (a) corepresentations contain only one representation of the unitary subgroup, and thus we have no new degeneracy. Type (b) corepresentations contain the same representation of the unitary subgroup twice, and new degeneracy may appear, while type (c) corepresentations contain two inequivalent correpresentations of the unitary subgroup, and thus we have a degeneracy.

We can now distinguish two cases of interest. We are interested in the two places on the Brillouin zone where we have the maximum symmetry, which translates to $k = 0$ and $k = pi/\Lambda$.

- $k = 0$ Here the set of symmetry operations is $M^{k=0} = (e, m, \xi, \mu) = N + AN$ where N is the unitary subgroup and A is an arbitrary antiunitary operator. Since k=0, $exp(i0n\Lambda) = 1$. Also squaring the antiunitary operators we get the identity operator and thus the character is 1 in both cases. So the test says that we have no degeneracy at k=0, because the corepresentations there, are

all of Type (a). Thus, Mock concludes that thresholdless $\mathcal{PT}$ degeneracy isn't expected to occur there. Which just means that we expect real eigenvalues on $k = 0$

- $k = \pi/\Lambda$ Here the space group representation is $e^{in\pi} = \pm 1$ in case n is even or odd. To take into account this fact we introduce the bar operators $\bar{e}, \bar{m}, \bar{\xi}, \bar{\mu}$ which are of the form $\{R|(2n+1)\Lambda + t\}$ while the previous ones are $\{R|2n\Lambda + t\}$ Now the unitary subgroup is of index 4 and our set is isomorphic to $C_{4\nu}$ while the unitary subgroup is isomorphic to $C_{2\nu}$. In this case $\mathcal{W} = (\xi, \bar{\xi}\mu, \bar{\mu})$ which when squared gives: $(\bar{e}, \bar{e}, e, e)$ Looking up the character of the isopmorphic group in a book we see that we have both Type(a) ant Type (c) corepresentations. However, it is Mock's argument that: "*Physically, we seek corepresentations that change sign upon application of e and* $\bar{e}$. Therefore he discards the type (a) which do not change sign. And thus concludes that at the edge of the Brillouin zone modes exhibit a thresholdless PT transition, we conclude that Type (c) 2D corepresentations are associated with thresholdless $\mathcal{PT}$-degeneracy and vice versa.

This, as we will show in the next chapters, does not hold true in our case. One of the assumptions that is different is that he is working with Hamiltonians with discrete spectrum and also with the Maxwell equations instead of the Schroedinger as we did.

Chapter 5

Numerical Methods

Before we continue with the analytical and numerical results of the thesis we would like to introduce the methods that were used to solve the equations of our problem.

As mentioned before one of the topics of the thesis is the band structure of non-Hermitian $\mathcal{PT}$-symmetric Hamiltonians. To find the band structure of a lattice Hamiltonian is to find the energy eigenvalues of the Hamiltonian for every different Bloch mode. Therefore we have to solve the Schroedinger equation for a periodic potential V(x). In the general case of potential the problem is not analytically solvable, and that is why we rely on computational methods. One of the methods is called Finite Differences Method.

5.1 Finite Differences Method (FDM)

To explain in detail this numerical method that was used to calculate the band structure of a one dimensional periodic potential ($V(x) = V(x + a)$) we will have as a starting point the linear paraxial equation of diffraction in the presence of a potential which is mathematically the same with the Schroedinger's Equation, which in the context of photonics is given in normalized units:

$$i\frac{\partial u}{\partial z} + \frac{\partial^2 u}{\partial x^2} + V(x)u = 0 \tag{5.1}$$

To determine the eigenmodes of the potential, we use the Ansatz:

$$u(x, z) = u(x)e^{i\beta z} \tag{5.2}$$

That way we eliminate the time (z) derivative and we get a linear eigenvalue problem. Now by applying the Floquet-Bloch theorem which is nothing more than decomposition of the field envelop into an infinite number of orthogonal modes ϕ_m which are

called Floquet Bloch modes:

$$u(x) = \sum_m \phi_m e^{ik_m x} \tag{5.3}$$

we can further simplify our task. So by putting Eqs. (5.2) and(5.3) in Eq. (5.1) we get:

$$\phi_m^{"} + 2ik_m\phi_m^{'} - k_m^2\phi_m + V(x)\phi_m = \beta\phi_m \tag{5.4}$$

Since the last relation holds true for all Bloch modes we can omit the m index for convenience. Also since our problem is periodic we can and are going to work in only one cell and impose periodic boundary conditions.

As you may have guessed this method is based on discretizing our space. This helps us write down the derivatives of ϕ as:

$$\phi^{'} = \frac{\phi_{i+1} - \phi_{i-1}}{2\Delta x}$$

$$\phi^{"} = \frac{\phi_{i+1} - 2\phi_i + \phi_{i-1}}{\Delta x^2}$$

where Δx is the distance between two discrete points in our space.

Substituting the last two expressions in Eq. (5.4) we get:

$$\left[\frac{1}{\Delta x^2} + \frac{ik}{\Delta x}\right]\phi_{i+1} + \left[\frac{1}{\Delta x^2} - \frac{ik}{\Delta x}\right]\phi_{i-1} + \left[V_i - k^2 + \frac{2}{\Delta x^2}\right]\phi_i = \beta\phi_i \tag{5.5}$$

The above equation describes a tridiagonal matrix eigenvalue problem. By defining A,B,C the coefficients in front of the $\phi_{i+1}, \phi_{i-1}, \phi_i$ respectively we can write down this equation as:

$$M \cdot \phi = \beta\phi \tag{5.6}$$

where M is a tridiagonal matrix [B C A] with the only non zero elements being the diagonal and the 1-off diagonal ones. So all we have to do is find the eigenvalues of M for every k in the first Brillouin zone$\left[-\frac{\pi}{a}, \frac{\pi}{a}\right]$ where a is the period of the lattice.

5.2 Plane Wave Expansion Method (PWE)

PWE is a computational method whose main purpose is to solve differential equations by formulating them to a corresponding eigenvalue problem. This method is very popular in condensed matter physics of periodic systems, as well as photonic crystal physics as a method to determine the band structure of a crystal.

Again the starting point will be Eq.(5.1)

$$i\frac{\partial\psi}{\partial z} + \frac{\partial^2\psi}{\partial x^2} + V(x)\psi = 0 \tag{5.7}$$

Again we use the ansatz (5.2) and the Floquet-Bloch theorem (5.3) but now instead of discretizing our space we use the assumption that the amplitudes of the Bloch modes are plane waves:

$$u = \sum_n p_n e^{-i\frac{2\pi n x}{a}} \tag{5.8}$$

and also our potential can be written in the form:

$$V(x) = \sum_m V_m e^{-i\frac{2\pi m x}{a}} \tag{5.9}$$

which is not a problem since our potential is periodic. Note that a is the period of our lattice.

Substituting all these in Eq.(5.7) and renaming the dummy variables inside the summing signs we get:

$$-\left(\frac{2\pi n}{a} + k\right)^2 p_n + \sum_m V_m p_{n-m} = E p_n \tag{5.10}$$

Again we can express the above equation as an eigenvalue problem.

Note that this semi-analytical method is exact up to the point we have to calculate the eigenvalues. And its precision depends only on the precision of the code that calculates the eigenvalues of a matrix.

5.3 Spectral Method for Beam Propagation (SMBP)

The study of wavepacket diffraction in an optical lattice defined by a periodic potential is not a trivial task. The method that we use for this task is the Spectral method. It is quite well known that the Maxwell equation for light propagation in a source-free, non-magnetic material under the paraxial approximation can be written in a Schroedinger-like form as:

$$i\partial_z\phi + \partial_{xx}\phi + +V(x)\phi = 0 \tag{5.11}$$

where one can imagine z as the corresponding temporal coordinate of Schroedinger Equation since we can arrange the lattice in such way so that the beam is propagated in the z direction. The numerical method we used is also applicable in the case

of the Non-Linear Schroedinger Equation (NLSE) which has the same form with the Gross-Pitaevskii equation used in the mean field theory approximation. These equations have a Kerr non-linearity in the form of $g|\phi|^2\phi$. The initial value problem with the non-linearity is in general not solvable analytically so that is why we proceed numerically.

We have to note here, that we focus on linear diffraction effects without taking into account any non-linear interactions. From the computational point of view, the treatment of the potential term is the same with the Kerr non-linear term.

The basic idea of this method is to find a transformation such that the linear part of the PDE is cancelled out in the Fourier space. In this way we can reduce the problem to a non-linear ODE in Fourier space and use the standard methods for solving them like for example the Runge-Kutta method. The transformation in question is actually an ansatz. We use the ansatz that the solution of the full problem would not be much different from the solution of the linear problem which is:

$$\phi(x,z) = \int \bar{\phi}(k,z_0)e^{-ik^2z}e^{ikx}dk \tag{5.12}$$

where we solved the one dimensional problem for simplicity. One can see that the $\bar{\phi}(k,z_0)$, which is the amplitude of the solution in the Fourier space, does not depend on z(time). Our ansatz is that we have the same form in the solution of the full problem but the amplitude now depends on z(time):$\bar{\phi}(k,z)$. Using now the proposed solution together with Eq.(5.11) with the non-linear term we get:

$$\frac{\partial\bar{\phi}}{\partial z} = ie^{ik^2z}\mathcal{F}\left\{[V(x)]\,\mathcal{F}^{-1}\left(\bar{\phi}e^{-ik^2z}\right)\right\} \tag{5.13}$$

Now we can solve the ODE in Eq.(5.13) with the Runge-Kutta method and once we are done we can Fourier transform the solution back to real space. That is why we call this method Spectral.

Chapter 6

Potentials with varying real and imaginary part

In this chapter we will use the notion of Pseudo-Hermiticity to find the exceptional points of the non-Hermitian potentials and study their spectrum. We will start with the general case with arbitrary n in Eq.(1.3). After that we will consider the specific case of $n = 2$ to see what happens to the band structure. Subsequently, we will examine the wave propagation of a wide Gaussian beam in such lattice Hamiltonians.

6.1 The $cos^{2n}x$ potentials

We want to study the lattice Hamiltonian with the potential given in Eq.(1.3):

$$V(x) = cos^{2n}(x) + i\sum_{m=1}^{m=n} V_{2m} sin(2mx) \tag{6.1}$$

since such potentials can describe semiconducting waveguide arrays. Experimentalists can fabricate semiconducting complex materials that are described by this kind of potentials. In the case of an arbitrary n we have n free parameters which we call V_{2m} and m varies from $m = 1$ to $m = n$. What we are going to do is to transform this potential in a way that enables us to see what would be the appropriate similarity transformation and under what linear automorphism this Hamiltonian can be Hermitian. We have the following:

$$\begin{aligned} cos^{2n}(x) &= \frac{1}{2^{2n}}\left(e^{ix} + e^{-ix}\right)^{2n} \\ sin(2mx) &= \frac{1}{2i}\left(e^{i2mx} - e^{-i2mx}\right) \end{aligned} \tag{6.2}$$

Now we can use the formula for the binomial expansion:

$$(x+y)^{2n} = \sum_{k=0}^{k=2n} \left(\begin{array}{c} 2n \\ k \end{array} \right) x^{2n-k} y^k \tag{6.3}$$

where the parenthesis is the binomial expansion coefficient and it is calculated by:

$$\left(\begin{array}{c} 2n \\ k \end{array} \right) = \frac{2n!}{(2n-k)!\, k!}$$

Applying Eq.(6.3) in the first relation of Eq.(6.2) we can see that the terms with $e^{\pm i(2n-2k)x}$ will have the same coefficients in front of them we can group together with the $sin(2n-2k)x$ terms. So by focusing on the term $2(n-k)$ to avoid the sums we have:

$$\begin{aligned} t_{2(n-k)} = \frac{1}{2^{2n}} \left(\begin{array}{c} 2n \\ k \end{array} \right) \left(e^{2ix(n-k)} + e^{-2ix(n-k)}\right) + \\ + \frac{V_{2(n-k)}}{2} \left(e^{2ix(n-k)} - e^{-2ix(n-k)}\right) \end{aligned} \tag{6.4}$$

We can rewrite Eq.(6.4) to look like:

$$\begin{aligned} t_{2(n-k)} = \frac{\left(\begin{array}{c} 2n \\ k \end{array} \right)}{2^{2n}} e^{i2x(n-k)} \left(1 + y_k\right) + \\ + \frac{\left(\begin{array}{c} 2n \\ k \end{array} \right)}{2^{2n}} e^{-i2x(n-k)} \left(1 - y_k\right) \end{aligned} \tag{6.5}$$

where

$$y_k = \frac{V_{2(n-k)} 2^{2n-1}}{\left(\begin{array}{c} 2n \\ k \end{array} \right)}$$

Before we continue, note that:

$$tanh^{-1}(x) = \frac{1}{2} ln \left(\frac{1+x}{1-x} \right) \tag{6.6}$$

and the fact that we can distinguish two cases depending on the sign of the second parenthesis in Eq.(6.5). So we have:

- *positive parenthesis.* Since our free parameter is the V_i's we must have:

$$V_{2(n-k)} < \frac{\left(\begin{array}{c} 2n \\ k \end{array} \right)}{2^{2n-1}} \tag{6.7}$$

Now we can use Eq.(6.6) to rewrite Eq.(6.5) as:

$$A_k\sqrt{1-y_k^2}cos\left(2x(n-k)-itanh^{-1}y_k\right) \tag{6.8}$$

where:

$$A_k = \left(\begin{array}{c} 2n \\ k \end{array}\right) 2^{1-2n}$$

- *negative parenthesis.* Now we have to take:

$$V_{2(n-k)} > \frac{\left(\begin{array}{c} 2n \\ k \end{array}\right)}{2^{2n-1}} \tag{6.9}$$

In this case Eq.(6.5) is written in this form:

$$iA_k\sqrt{y_k^2-1}sin\left(2x(n-k)-itanh^{-1}\left(\frac{1}{y_k}\right)\right) \tag{6.10}$$

Now that we have the final transformed form of our $2(n-k)^{th}$ term of our potential we can start looking for automorphisms such that the Hamiltonian obeys the pseudohermiticity condition. One can actually guess the transformation from Eq.(6.8). We want to make a transformation that cancels out the imaginary part in the cosine. Well, that is an easy task, since:

$$e^{-\theta p}xe^{\theta p} = x + i\theta, \quad e^{-\theta p}V(x)e^{\theta p} = V(x+i\theta) \tag{6.11}$$

where x is the position operator, p is the momentum operator and θ is a parameter that we can tune so as to eliminate the $itanh^{-1}$ term. The appropriate θ is:

$$\theta = \frac{1}{n-k}tanh^{-1}y_k \tag{6.12}$$

And now one can see that if we are in the *positive parenthesis* case $V^*(x) = e^{-\theta p}V(x)e^{\theta p}$ while in the *negative parenthesis* case $V^*(x) \neq e^{-\theta p}V(x)e^{\theta p}$. So we have arrived at the conclusion that if condition (6.7) holds then our Hamiltonian is pseudohermitian and as such has a real spectrum.

However we have to satisfy similar equations for θ for $n-1$ more terms since k can take values from 0 to $n-1$. So we will have n equations of the form of (6.12). By eliminating the free parameter θ that was introduced later in the analysis we have $n-1$ equations of the form:

$$\frac{1}{n}tanh^{-1}y_0 = \frac{1}{n-1}tanh^{-1}y_1 = ... = tanh^{-1}y_{n-1} \tag{6.13}$$

To sum up we have n free parameters to determine and only n-1 equations. This means that there is a solution for those parameters it will always be on a line on the whole n-dimensional parameter space. One should note that the parameters should satisfy both Eq.(6.7) and Eq.(6.13). Under these conditions the eigenvalue spectrum of the Hamiltonian will always be real on the aforementioned line in the parameter space. Here we have shown that the critical point-condition depends on the difference on the power of the real and imaginary parts. One can also see that the reality of the spectrum highly depends on the existence and suitability of the real part of the potential.

6.2 Example: The $n = 2$ case

Since the case n=1 has been studied extensively both numerically [5] and analytically [6], to acquire more intuition about the problem we will use the formulae that we derived above to study the simple case of:

$$V(x) = cos^4 x + iV_2 sin(2x) + iV_4 sin(4x) \tag{6.14}$$

In the Fig.6.1 is depicted the real and imaginary parts of the potential in the n=2 case. In this case n=2 and k can take only the values 0 and 1. In this case our

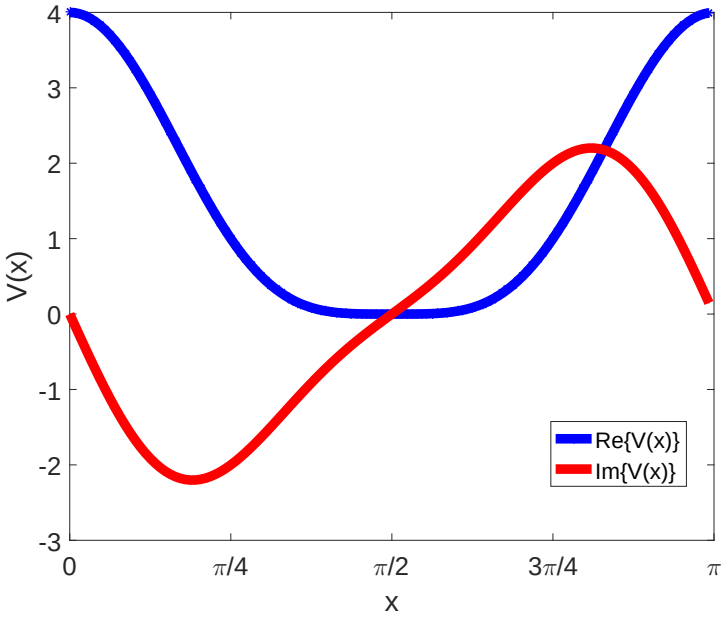

Figure 6.1: The potential of Eq.(6.14) with $V_2 = 0.5$ and $V_4 = 0.125$

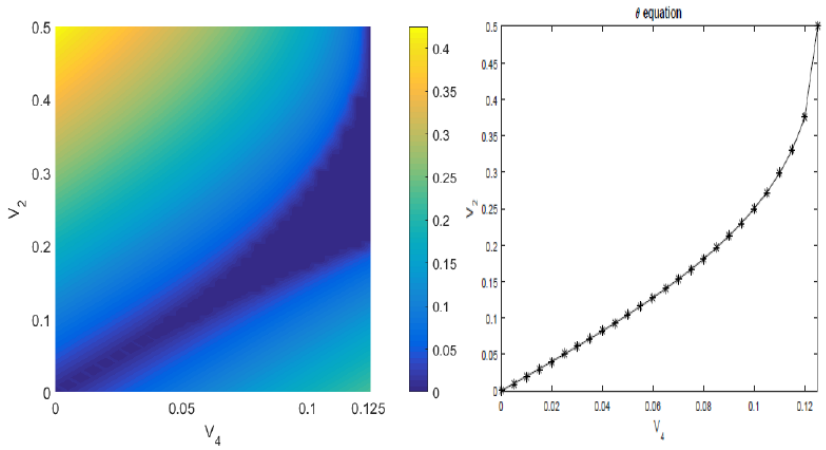

Figure 6.2: The 2d map of the parameter space. One can actually verify that the line described by Eq.(6.16) is inside the dark blue sector.

potential can be written in the following form:

$$V(x) = \begin{cases} 3 + Ac(2x - ith^{-1}2V_2) + Bc(4x - ith^{-1}8V_4), a \\ 3 + Ac(2x - ith^{-1}2V_2) + iBs(4x - ith^{-1}\dfrac{1}{8V_4}), b \\ 3 + iAs(2x - ith^{-1}2V_2) + Bc(4x - ith^{-1}8V_4), c \\ 3 + iAs(2x - ith^{-1}\dfrac{1}{2V_2}) + iBs(4x - ith^{-1}\dfrac{1}{8V_4}), d \end{cases} \tag{6.15}$$

where c stands for cos, s stands for sin, th stands for tanh and a,b,c,d correspond to the cases:

- a : $V_2 < 0.5$ and $V_4 < 0.125$
- b : $V_2 < 0.5$ and $V_4 > 0.125$
- c : $V_2 > 0.5$ and $V_4 < 0.125$
- d : $V_2 > 0.5$ and $V_4 > 0.125$

while the condition that needs to be satisfied so as to have real eigenvalue spectrum in the case a is:

$$8V_4 = tanh(2tanh^{-1}2V_2) \tag{6.16}$$

This is also partially verified by numerical analysis of the potential as shown in the figure Fig.6.2. We used the Plane Wave Expansion method to solve the Schroedinger's equation numerically and make a 2 dimensional map. In the figure we can see the maximum value of the imaginary part of the energy for all Bloch wave numbers(κ is

the normalized Bloch wave number.) and all energy bands. In the two axes we have our parameters V_2 and V_4. This is a map of the 2 dimensional parameter space. As one can see we have a surface of zero maximum imaginary part which grows as V_4 grows. However one should note that the Eq.(6.16) is inside the surface.

To acquire further intuition concerning the potential, we have studied the band structure and the behaviour of the bands in the case of vanishing V_2 and vanishing of V_4.

- $V_2 = 0$ In this case we vary V_4. As you can see in the Fig.6.3, that have been

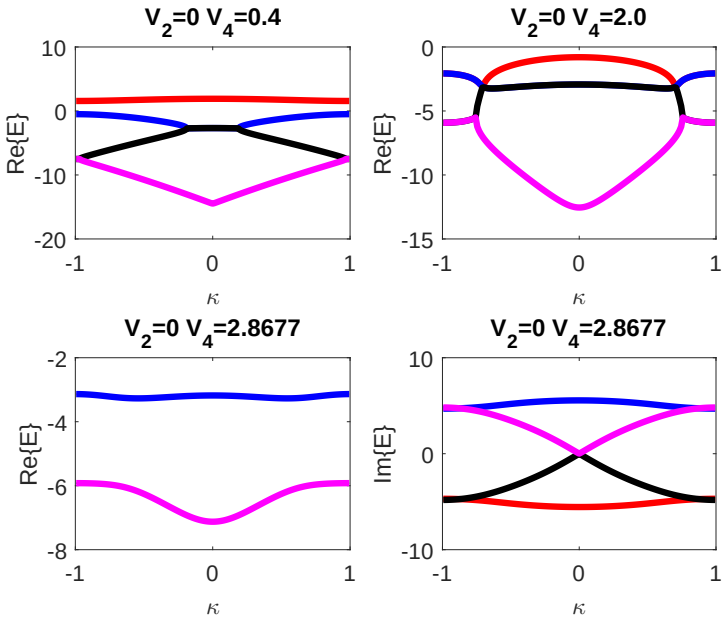

Figure 6.3: The band structure in the first case. The $1^{st}, 2^{nd}, 3^{rd}$ and 4^{th} bands correspond to the lines with red, blue, black and magenta color respectively.

acquired using the Plane Wave Expansion method (PWE) as we turn V_4 on we have an overlap between the second and the third band at the center of the Brillouin zone and another merging between bands number 3 and 4 at the edge of the Brillouin zone. As V_4 grows the first two bands merge at $V_4 \sim 1.55$ and in the limit of large $V_4 \sim 2.8675$ bands 1 and 2 become the same while the 2^{nd} and 3^{rd} become different and 3^{rd} and 4^{th} also are the same band.

- $V_4 = 0$ In this case we vary V_2. Utilizing the same method we plotted the band structure for V_2 0.4, 0.8 and 1.0. As we can also see in the diagram below we start with an overlap between the second and third band and while V_2 is growing,

it appears a merging of the first and second bands which finally surmounts and negates the overlap between the second and third bands at $V_2 = 1$.

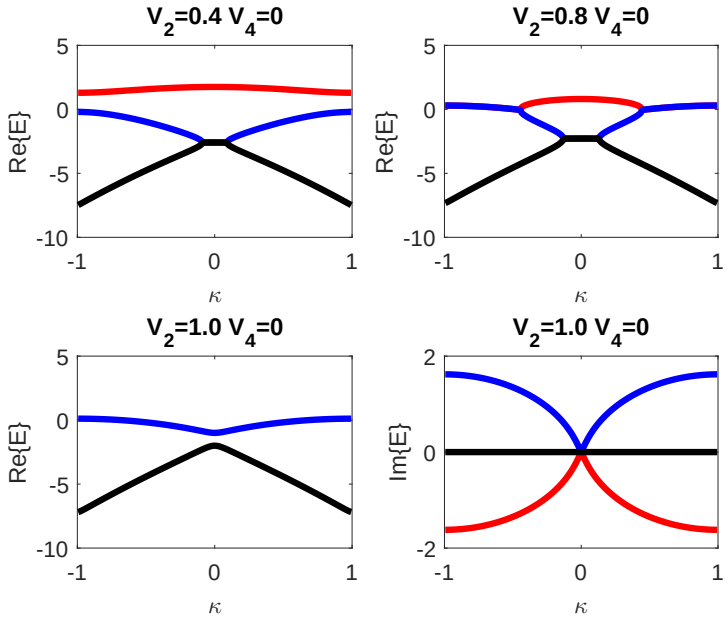

Figure 6.4: The band structure in the second case. Again here, the red line corresponds to the 1^{st} Band the blue line to the 2^{nd} Band, while the black line to the 3^{rd} Band.

6.3 Wavepacket Diffraction Dynamics

In this section we will study the beam propagation in an optical lattice defined by the potential we introduced in the section 6.2. The method that we applied is the Spectral method which was introduced in the previous chapter.

The plots in Fig. 6.5 depict the propagation of a Gaussian beam in an optical Lattice made by an array of waveguides which are constructed so that they are governed by the potential we just introduced. In 6.5(a) the Gaussian beam is narrow enough to excite only an individual channel, and thus we call it single excitation while in 6.5(b) the Gaussian beam is wide enough to excite much more channels. As we can see in both cases we are in the exact $\mathcal{PT}$ regime since we see this unexpected asymmetric diffraction pattern of these $\mathcal{PT}$ optical lattices. This assymetric pattern stems from the asymmetry of the imaginary part of the refractive index, namely the loss inside a channel resides on the right side. One can think that the openess of our system leads to energy flow from the gain towards the lossy regions. Intuitively

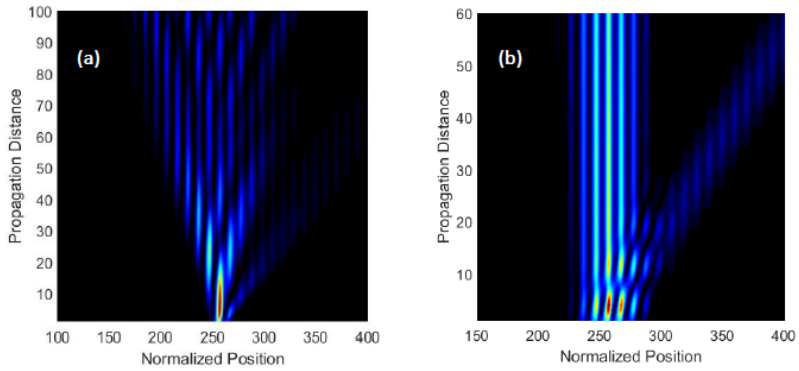

Figure 6.5: The dynamic evolution of optical field as the beam is propagated in the z direction(y-axis of plot) and one (b) or many waveguides are excited (a). In the figure we plotted the evolution of the optical field for $V_2 = 0.49$ and $V_4 = 0.125tanh(2atanh(2V_2))$ in the potential of the previous section.

this can also be seen as gain and loss dipoles, which promote energy flow from left to right thus from gain to loss. Another feature associated with beam propagation is power oscillation. In this case the quantity that is conserved is the quasipower introduced in [9], instead of the physical power which oscillates during propagation. This phenomenon is augmented under single channel excitation.

One can see that we have many interesting and counterintuitive behaviors. Similar results have been found in [5].

Chapter 7

Potentials with Varying Imaginary Part

In this chapter we are going to investigate potentials with a fixed real part and an imaginary part of varying spatial frequency. Here we consider the real part to be cos^2x which has a period of π. If we take as the imaginary part the functions $sin(nx)$ then we can distinguish two cases depending on the result of the integral:

$$I = \int_{cell} Im\{V(x)\}dx \tag{7.1}$$

If I is 0 then this means that n is an even number while non-0 means that n is odd. We are going to examine in detail both cases separately.

- $I = 0$: In this case we have the same amount of gain and loss in a single cell of our lattice. As one could intuitively guess things are better when we have the same amount of gain and loss (on average) in one cell. We may have not have a regime where our parameter makes the eigenvalue spectrum entirely real but we have some intriguing properties. It is known by [5] that in the case of $V(x) = cos^2x + iV_2sin2x$ that we have a critical point at $V_2 = 0.5$ and that after that point the first 2 bands merge and become degenerate. According to our reuslts, the bands that will merge first and will be physically relevant will be n and $n+1$ if the imaginary part is written as such $V_{2n}sin(2nx)$. However, as one can also glean from the figures Fig.7.2 there is a quite small overlap between the fourth and fifth band which is in the center of the Brillouin zone and only for $\kappa = 0$ independently from the value of our parameter. This leads us to believe that it is irrelevant. In the figure we can see the merged bands in the case of n=2 and n=3. We can also see that we may have thresholdless $\mathcal{PT}$-symmetry breaking but the degeneracy in the case of $sin(4nx)$ happens in the middle of the

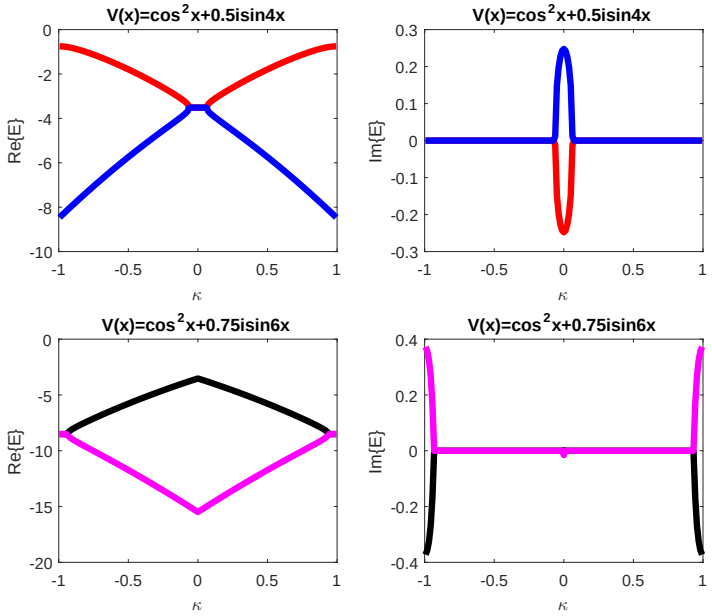

Figure 7.1: The bandstructure in the first case. In the first pair of plots the with the red line is depicted the 2^{nd} Band while with the blue line the 3^{rd}. Below, black is used for the 3^{rd} Band and magenta for the 4^{th} Band

Brillouin zone. This comes to a disagreement to [8], something to be expected since he was considering discrete spectrum in his work. Before we proceed, note that in Fig.7.3 the values of the imaginary part of the propagation constants (energy eigenvalues in quantum mechanics) are not 0 but of order 10^{-7}.

- $I \neq 0$ In the case at hand we don't have the same amount of gain and loss in one cell. Here as we can see, the merging of the bands happens only at the edge of the Brillouin zone. We also see the same behaviour, that the first bands to merge are the n and $n+1$ in the case we write our imaginary part as $sin(nx)$ where n is odd. However in this case the overlap between lower bands remains.

Finally, in the last two figures one can see the behaviour of the maximum imaginary part of the propagation constants (energy eigenvalues) of the whole lattice as we increase the amplitude of gain-loss. In the second case we have a linear relation while in the first case there is a more violent first order phase transition-like relation. This happens for every $sin(2nx)$ imaginary part except for the case of $n = 4$. That is because there exist the small degeneracy of 4th and 5th band for all $n \leq 4$.

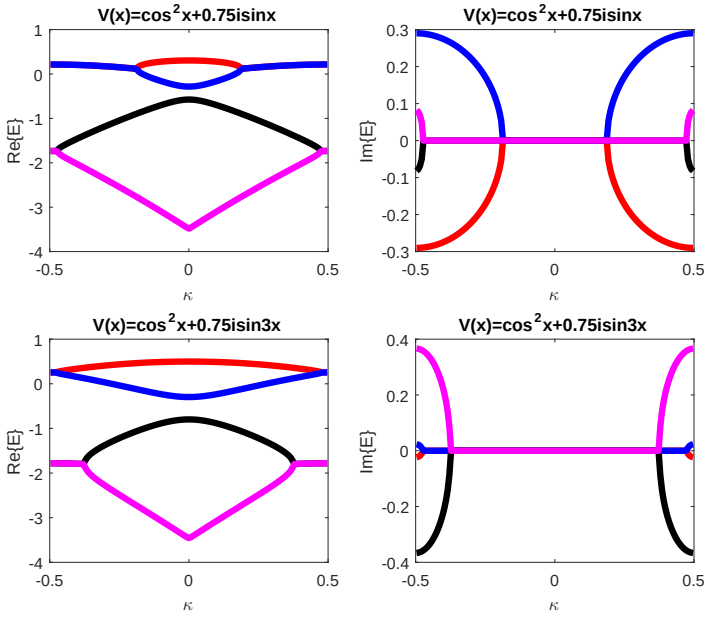

Figure 7.2: The bandstructure in the second case. With red we represent the first band, with blue the second band and the 3^{rd} and 4^{th} bands with black and magenta respectively.

7.1 Wavepacket Diffraction Dynamics

In this section we will study the beam propagation in an optical lattice defined by the potential we introduced in this chapter. For obvious reasons we examine potentials with $I = 0$. The results were obtained for the potential

$$V(x) = 4(cos^2 x + iV_4 sin4x)$$

. This potential is as shown previously in the $\mathcal{PT}$-broken phase. However, it is the modes belonging to the second and third bands that break the $\mathcal{PT}$-symmetry. Thus we would expect that under single mode excitation the power to look like in Figure 7.5 while under wide beam excitation we expect to have an exponential increase in power as the beam propagates. Since we are in the broken $\mathcal{PT}$-symmetry regime all the energy would go to the gainy sites and thus the energy would not be conserved. And that is indeed what we see in the figure below.

One can see that as we increase n in $sin(2nx)$ the modes that break the symmetry become more and more physically irrelevant since these modes are of higher and higher energy,which experimentally is a difficult if not impossible task to excite.

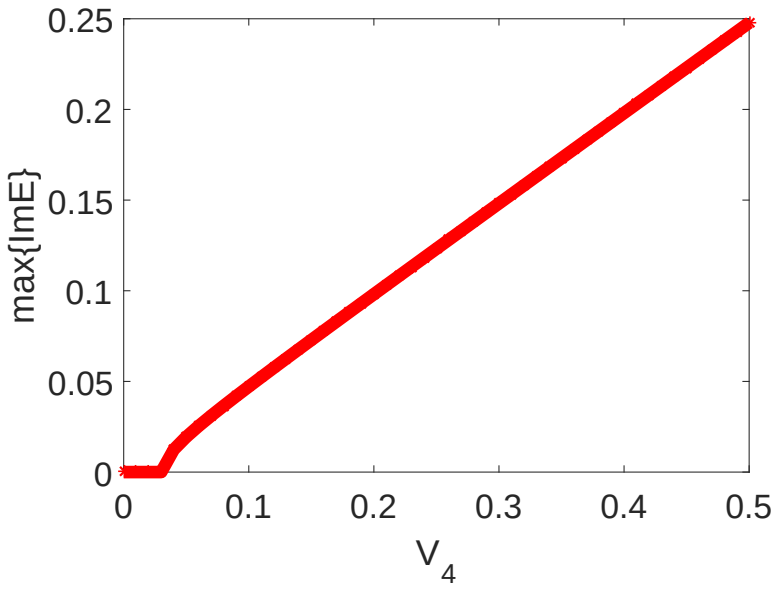

Figure 7.3: The maximum imaginary part of the Energy eigenvalue in the whole lattice for $V(x) = cos^2 x_i V_1 sin4x$.

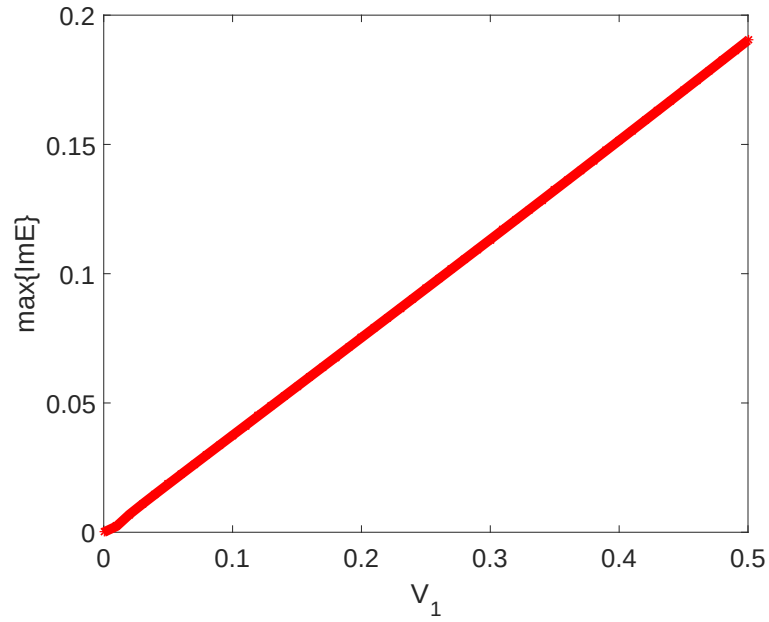

Figure 7.4: The maximum imaginary part of the Energy eigenvalue in the whole lattice for $V(x) = cos^2 x_i V_1 sinx$.

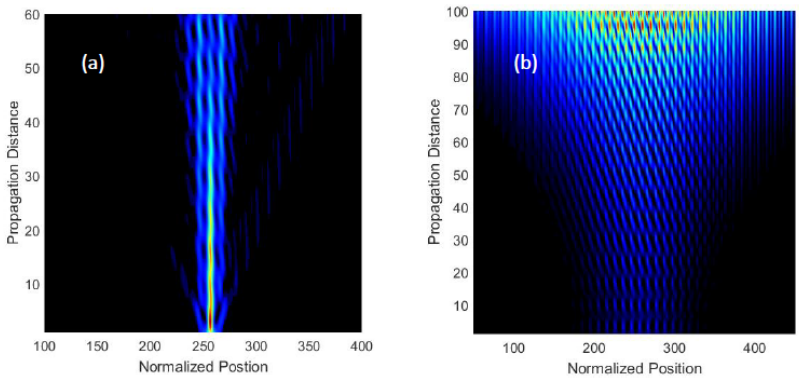

Figure 7.5: The dynamic evolution of the optical intensity as the beam propagates in the z direction(y-axis of plot) under single (a) channel exciation, and (b) under wide gaussian beam excitation. In the figure we plotted the evolution of the optical intensity for $V_4 = 0.15$ for the potential.

Chapter 8

Conclusions and Discussion

In conclusion, we have studied novel classes on non-Hermitian Hamiltonians that respect $\mathcal{PT}$-symmetry. More specifically we used the notion of Pseudo-Hermiticity to analytically predict a critical "line" in the parameter space on which we have real eigenvalues. We showed that what determines the critical point-condition is the difference in power of the imaginary and real part of the non-Hermitian potential and that the real part of the potential is crucial to the existence of such a point-condition.

Finally, we have studied potentials without changing the real part of the potential and concluded that when the gain and loss is balanced on average in a cell of a lattice we have a more violent transition in the imaginary part of the propagation constants and that the faster the oscillations in the imaginary part the higher are the bands that merge(and have complex conjugate pairs of energy eigenvalues). Since our excitation beam has finite energy and width, it can excite mostly Floquet-Bloch modes in the first three bands. Therefore we can construct a wide class of PT-lattices with their first three bands unbroken for a wide range of gain-loss amplitudes.

References

[1] C. M. Bender and S. Boettcher, Phys. Rev. Lett. **80**, 5243 (1998).

[2] C. M. Bender, S. Boettcher and P. N. Meisinger, J. Math. Phys. **40**, 2201 (1999).

[3] C. M. Bender, D. C. Brody and H. F. Jones, Phys. Rev. Lett.**89**, 270401 (2002).

[4] R. El-Ganainy, K. G. Makris, D. N. Christodoulides and Z. H. Musslimani, Opt. Lett. **32**, 2632 (2007).

[5] K.G. Makris, R El-Ganainy, D.N. Christodoulides and Z.H. Musslimani, Phys. Rev. Lett. **100**, 103904 (2008).

[6] B. Midya, B. Roy and R. Roychouhury, Phys. Lett. A **374**, 2605 (2010).

[7] A. Mostafazadeh, J. Math. Phys., Vol. **43**, No. **1**, 205 (2002).

[8] A. Mock, Optics Express, Vol. **24**, No. **20**, 22694 (2016).

[9] B. Bagchi, C. Quesne, and M. Znojil, Mod. Phys. Lett. A **16**, 2047 (2001).

[10] A. P. Cracknell, *Group Theory in Solid-State Physics*, Taylor and Francis, London, (1975).

[11] E. P. Wigner, *Group Theory and its Application to the Quantum Mechanics of Atomic Spectra*, Academic Press, (1959).

[12] M. Tinkham, *Group Theory and Quantum Mechanics*, Dover Publications, (1964).